ROSAT X–RAY OBSERVATIONS OF STELLAR FLARES: UV CET TYPE STARS OF THE SOLAR VICINITY

V. Hambaryan[1,2], R. Neuhäuser[2], B. Stelzer[2], and A. D. Schwope[1]

[1] *Astrophysikalisches Institut Potsdam, An der Sternwarte 16, 14482 Potsdam, Germany*
e-mail: vhambaryan@aip.de

[2] *Max-Planck Institute für Extraterrestrische Physik, D-85740 Garching bei München, Germany*

We present the results of a comprehensive survey of X-ray observations of flare stars in the solar neighborhood carried out with the *ROSAT* satellite. The data sample comprises 525 PSPC and 149 HRI pointed as well as *ROSAT* All-Sky (RASS) survey observations pertaining 143, 69 and 463 stars, respectively, from the catalogue of UV Cet type stars and related objects of Gershberg *et al.* [1]. In total, the sample represents nearly 1350 hours monitoring of flare stars at X-ray wavelengths (0.1–2.4 KeV). The timing analysis of the data has been performed by Scargle's [2] change point detection method using Bayesian model comparison technique, directly applicable to the unbinned data. We present results of brightness variations corresponding to the 94 PSPC, 40 HRI and 26 RASS detections. Both quiescent and flare emission is estimated and hardness ratios for PSPC observations are presented. For 9 comparatively powerful flares observed by the PSPC, time resolved spectroscopy is presented clearly indicating an increase of coronal metallicity abundance at flare maximum.

INTRODUCTION

The discovery and study of red dwarf flare stars (FSs) in the solar vicinity and in star clusters and associations had a fundamental significance for the study of the physics and evolution of red dwarf stars.

Stellar flares represent one of the most challenging problems of contemporary astrophysics. Both solar and stellar observations have shown the flare phenomenon to be very complex, and in recent years important progress has been made from observations over wide wavelength ranges.

FSs were discovered in the late 1940s in the solar vicinity and named UV Cet type variables (classical FSs). According to a recent definition by Gershberg *et al.* [1], these stars are on the lower part of the main sequence and show phenomena inherent to solar activity (sporadic flares, dark spots, variable emission from chromospheres and coronae, radio, X-ray and UV bursts). At present, the total number of known UV Cet type stars is 463 (Gershberg *et al.* [1]).

Further, systematic investigations of stellar flares in nearby stellar clusters (*e.g.*, Pleiades) and associations (*e.g.*, Orion) have revealed a fundamental significance of this phenomenon for the physics and evolution of the young low-mass stars and protostars (see, *e.g.*, Mirzoyan [3], Montmerle [4]). At present, the observations of stellar flares at different wavelengths of the electromagnetic spectrum has become a scientifically productive area of astrophysics.

In the 1970s, the first X-ray studies of stellar flares were made, in particular with the *Einstein Observatory* (*EO*) (1978–1981) and the *EXOSAT* Observatory (1983–1985). Comprehensive reviews of the *EO* observations of stellar X-ray flares are presented by Haisch [5] and of the *EXOSAT* observations by Pallavicini, Stella & Tagliaferri [6]. X-ray observations of some stellar flares obtained during the *ROSAT* All-Sky Survey as well as in *ROSAT* pointings are discussed by Schmitt [7].

However, to date no systematic investigation of flare stars and stellar flares based on *ROSAT* observations has been done. X-ray observations by *ROSAT* are very well suited for statistical examination: Several physical quantities of individual X-ray photons are registered, namely the time of photon arrival, the direction of incidence, and the photon energy.

On the other hand, the wide spread timing analysis methods of datasets based on time binning technique give rise to certain difficulties: First of all, one has no a priori knowledge of the relevant timescales of a given flare to be detected, and, therefore, many different binnings of the data have to be considered; second, the bins must be large enough so that there will be enough photons to provide a good statistical sample, while larger bins will dilute short flares; moreover, the common practice of binning data overlooks a considerable amount of information and introduces a dependency of results on the sizes and locations of the bins. Meanwhile, it has been known for some time (Cash [8]) that fitting models to unbinned data is quite straightforward (see, for discussion, Scargle & Bapu [9]).

Hence, it is worthwhile to examine the available observational data of *ROSAT* in a straightforward and systematic way for variability testing, in particular, for UV Cet type flare stars.

For the flare event detection, we shall use the method described by Scargle [2] based on Bayesian statistics due to the nearly ideal Poisson nature of photon registration by the *ROSAT* detectors (Trümper [10], Pfeffermann *et al.* [11]).

In this article we will try to address various items relevant to detections and studies of flares with *ROSAT*.

1. DATA REDUCTION AND RESULTS

Details of our data reduction procedure have been described by Hambaryan *et al.* [12], (HNS) and briefly are as follows: from *ROSAT* PSPC and HRI pointed observations, as well as All-Sky Survey data in the direction of each optically known UV Cet type star we have extracted all photon events registered within a radius corresponding 0.95 quantile of the point spread function for the corresponding detector (Zimmermann *et al.* [13]). As a background for a given source the data from a nearby sector are used (HNS).

1.1 VARIABILITY TESTING

As mentioned in the introduction, for flare event detection we have used a method developed by Scargle [2] based on Bayesian statistics. The method is applicable to data that are known to be from a nearly ideal Poisson process, *i.e.*, a class of independent, identically distributed processes, having zero lengths of dead time.

The data gathered in *ROSAT* observations (telescope+detector) allow the measurement of arrival times of individual X-ray photons to the nearest $\approx 10^{-4}$ s (*i.e.*, an accuracy which is much smaller than the shortest time scales that are considered to be responsible for flare events on stars). Another departure from Poisson ideal distribution of counts is related to the detectors finite dead time (see, for discussion, Scargle & Bapu [9]).

Nevertheless, the arrival times of photons registered by *ROSAT* and presented in the so-called Photon Events Tables in this context can be considered as close to a Poisson process, *i.e.*, the arrival of a photon in any interval is independent on that in any other non-overlapping one.

Scargle's [2] method is designed for application to photon counting data and uses it for decomposition into a piecewise constant Poisson process. For example, let's assume that during a continuous observational interval of length T, consisting of m discrete moments in time, at which it was possible to make measurements (spacecraft's "clock ticks" $m = T/\delta t$), a set of photon arrival times D $(t_i, t_{i+1}, ..., t_{i+n})$ is registered. Suppose now that we want to use these data to compare two competing hypotheses. The first hypothesis is that the data are generated from constant rate Poisson process (model M_1) and the second one from two-rate Poisson process (model M_2). Evidently, model M_1 is described by parameter ν of one rate Poisson process while the model M_2 by parameters ν_1, ν_2 and τ describing two different parts of dataset D divided by any point τ from observational interval T (with lengths T_1 and T_2) at which the Poisson process switches from parameter (count rates) ν_1 to ν_2.

By taking as a background information (I) the proposition that one of the models under consideration is true and by using Bayes' theorem we can calculate the posterior probability (the probability that M_k $(k = 1, 2)$ is the correct model) of each model by (see, *e.g.*, Jaynes [16])

$$P(M_k|D,I) = \frac{P(D|M_k,I)}{P(D|I)} P(M_k|I) \tag{1}$$

where $P(D|M_k, I)$ is the (marginal) probability of the data given M_k, and $P(M_k|I)$ is the prior probability of model M_K $(k = 1, 2)$. The term in the denominator is a normalization constant, and we may eliminate it by calculating the ratio of the posterior probabilities instead of probabilities directly. Indeed, the extent to which the data support model M_2 over M_1 is measured by the ratio of their posterior probabilities and is called posterior odds ratio

$$O_{21} \equiv \frac{P(M_2|D,I)}{P(M_1|D,I)} = \left[\frac{P(D|M_2,I)}{P(D|M_1,I)}\right] \left[\frac{P(M_2|I)}{P(M_1|I)}\right]. \tag{2}$$

The first factor on the right-hand side of Eq. (2) is the ratio of the *integrated* or *global* likelihoods of the two models and is called the *Bayes factor* for M_2 against M_1, denoted by B_{21}. The global likelihood for each model can be evaluated by integrating over nuisance parameters and the final result for discrete Poisson events can be represented by (see, for details, Scargle [2])

$$B_{21} = \frac{1}{B(n+1, m-n+1)} \sum B(n_1+1, m_1-n_1+1) \times B(n_2+1, m_2-n_2+1) \Delta\tau \tag{3}$$

where B is the *beta function*, n_j and $m_j, (j = 1, 2)$, are the number of recorded photons and the number of "clock ticks" in the observational intervals of lengths T_1 and T_2, respectively, $\Delta\tau$ is the time interval between successive photons, and the sum is over the photons' index.

The second factor on the right-hand side of Eq. (2) is the prior odds ratio, which will often be equal to 1 (see below), representing the absence of a priori preference for either model.

It follows that the Bayes factor is equal to the posterior odds when the prior odds is equal to 1. When $B_{21} > 1$, the data favor M_2 over M_1, and when $B_{21} < 1$ the data favor M_1.

If we have calculated the odds ratio O_{21}, in favor of model M_2 over M_1, we can find probabilities for model M_2 by inverting Eq. (2), giving

$$P(M_2|D, I) = \frac{O_{21}}{1 + O_{21}}. \tag{4}$$

Applying this approach iteratively to the observational data set, the Scargle [2] method returns an array of rates, $(\lambda_1, \lambda_2, ..., \lambda_{cp})$, and a set of so-called "change points" $(\tau_1, \tau_2, ..., \tau_{cp-1})$, giving the times when an abrupt change in the rate is determined, *i.e.*, a significant variation. This is the most probable partitioning of the observational interval into segments during which the photon arrival rate was discernibly constant, *i.e.*, had no statistically significant variations. Unlike most, this method does not stipulate or predetermine time bins – instead the data themselves determine an effective, non-uniform binning in time. Therefore, this data analysis procedure does not itself impose a lower limit to the time scale on which variability can be detected. There are two free parameters in the method that are used to halt the segmentation process: The first is the minimum number of events that are allowed in a block (we have chosen two) and the second is a prior odds ratio that may be applied to disfavor segmentation. The prior odds ratio (second factor in the right-hand side of Eq. (2)) represents the relative likelihood assigned to the two models before the data is considered. Although this would appear to warrant a value of unity, in practice a larger value is used to prevent the method from making an incorrect decision to segment when two models are almost equally likely.

To have strong evidence in favor of segmenting, Scargle [2] suggests to use as a prior odds ratio a quantity which is equal to the ratio of the length of the observational interval and the desired time resolution of the data. For interpreting *Bayes factors* (B_{21}) considered above, there are some rules of thumb for evidence of model M_2 against M_1 (Jeffreys [17], Raftery [18]). Furthermore, it should be noted that this point is not crucial – we find very similar results independent on the choice of the prior odds ratio.

As it is well known, owing to the spacecraft orbits, *ROSAT* pointing observations contain data gaps. The integrated likelihoods that are used to decide between the above mentioned models M_1 and M_2 do not depend on the photon arrival times, only on the number of observing time resolution elements (number of *ROSAT* "clock ticks"), and the number of registered photons in the observational interval (see Eq. (3)). Therefore, in this context, the correct treatment of data gaps is to ensure that the gap length is not counted in the number of "clock ticks" (numbers m_j in Eq. (3)). In the case of *ROSAT* pointed observations by PSPC or HRI, we allowed to take into account this point with a special descriptor available in the Photon Events Tables (see Zimmermann *et al.* [13]).

Application of the above described procedure to the *ROSAT* archived data revealed in total 160 significant brightness variations corresponding to the 94 PSPC, 40 HRI and 26 RASS detections.

In order to estimate flare parameters we have converted the observed count rates to the fluxes and luminosities for each segment subtracting background and radiation of the star in the quiescent level.

The count rates of the flare in each energy band are expressed as

$$X_{Band}(t) = [X_{Flare}(t) + X_0]/X_0 - 1, \tag{5}$$

where X_0 is the quiescent star radiation count rates in the particular energy band, determined from data outside the flare event. This quantity can be used to determine the so-called equivalent duration of the flare

$$X_{ED} = \sum X_{Band}(t_k)\Delta t_k, \tag{6}$$

where $X_{Band}(t_k)$ is given by Eq. (5) for each kth segment. $X_{Band}(t_k)$ expresses the energy of the flare in terms of the quiescent star's energy.

An estimate of the luminosity of the quiescent star, in each band, can be made by multiplying count rates by an energy conversion factor and taking into account the distance of the star. Assuming that the spectrum of the star in the quiescent level is consistent with a one-temperature Raymond-Smith spectrum (Raymond & Smith [19]), a thermal spectrum from an hot, optically thin plasma of solar abundance, we use 1 KeV, *i.e.*, $\sim 10^7$ K, as temperature of the X-ray emitting plasma, which is typical for late-type stars (Neuhäuser *et*

Table 1: Distribution of detected flares in different energy bands for *ROSAT* PSPC pointed observations on the UV Cet type stars

ROSAT PSPC energy band	Number of flares
Broad-Soft-Medium-Hard	32
Broad-Soft-Medium	2
Broad-Soft-Hard	4
Broad-Medium-Hard	11
Broad-Hard	23
Only Broad	22
Total	94

al. [14]). Because foreground absorption is negligible for our objects, we use an energy conversion factor of 10^{-11} cts cm^2 erg^{-1} (Zimmermann *et al.* [13]) for the PSPC observation.

Furthermore, flare detection and parameter estimation procedures have been applied to different energy bands. Namely, the so-called hardness ratios (X-ray colors) which are defined as follows: if $X_{s,m,h}$ are the count rates in the soft (0.1 to 0.4 KeV), medium (0.5 to 0.9 KeV), and hard (0.9 to 2.0 KeV) bands, respectively, then

$$HR\,1 \;=\; \frac{X_h + X_m - X_s}{X_h + X_m + X_s} \quad \text{and} \quad HR\,2 \;=\; \frac{X_h - X_m}{X_h + X_m}$$

with this definition hardness ratios range from -1 to $+1$. If no counts are detected, *e.g.*, in the soft band, then HR1=1, but one can estimate a lower limit to HR1 by using the upper limit to the soft band count rate X_s in the formula above. These quantities have been computed for different observational phases, *i.e.*, for the star in the quiescent level as well as for flare radiation alone.

Many flares have been detected in different energy bands of the *ROSAT* PSPC observations. In Table 1 a summary of detected variations in different energy bands for *ROSAT* PSPC pointed observations are presented.

Mutual dependences between flare luminosities $\log L_X$ in different energy bands for *ROSAT* PSPC pointed observations are represented by simple proportionality relations:

$$\begin{array}{llll}
\log L_B = 0.994 \log L_S + 0.511, & \rho = 0.985 & \log L_B = 1.016 \log L_M + 0.377, & \rho = 0.963 \\
\log L_B = 1.056 \log L_H - 0.832, & \rho = 0.979 & \log L_H = 0.903 \log L_S + 2.431, & \rho = 0.969 \\
\log L_H = 1.025 \log L_M - 0.617, & \rho = 0.988 & \log L_M = 0.888 \log L_S + 2.738, & \rho = 0.952
\end{array} \qquad (7)$$

where index “B” corresponds to the broad, “S” – soft, “M” – medium, “H” – hard band as defined above and ρ is the coefficient of the correlation.

In Fig. 1 hardness ratios (HR2 versus HR1) of detected flares (filled circles) and corresponding stars (open circles) are shown. Note that flare radiation corresponds to the segment having maximum count rate.

1.2 SPECTRAL ANALYSIS

Since we do not have a sufficient number of counts for a detailed study of the evolution of the coronal temperature for most of the detected flares, we performed a spectral fit for the brightest of them (comparatively powerful ones) using a one temperature (1-T) Raymond-Smith (RS) model (Raymond & Smith [19]) including a photoelectric absorption term using the Morrison & McCammon [20] cross sections. Since the absorption for investigated objects is negligible (they are in the solar vicinity) we allow the parameter N_H to vary in the range $10^{18} - 10^{19}\,\mathrm{cm}^{-2}$. The abundance was left free. We fit the data for different time intervals: namely, for segments corresponding to Bayesian blocks (*i.e.*, in the time intervals within which data can be thought of being as generated from single rate Poisson process). These blocks were selected using the minimum number of photons for each segment equal to 500 as a halting rule (together with prior odds-ratio equal to 1) for further desegmentation (see Scargle [2], HNS).

Spectral fits have been performed using the XSPEC V10.0 package. Although abundances in stellar coronae in all cases show lower values than solar one, (an issue which is still debated; see, *e.g.*, Sciortino *et al.* [21]) these results are *not* to be interpreted as a measurement of abundances in the flare emission of these stars, since lower resolution X-ray measurements tend to have a bias toward lower abundances (*cf.* Schmitt *et al.* [22]). However, our results are consistent with an independent determination by Sciortino *et al.* [21] (*e.g.*, EV Lac) and may serve for comparative analysis of metal abundances during the evolution of a flare (the same initial values of the parameters of a model were used for different time intervals and different stars).

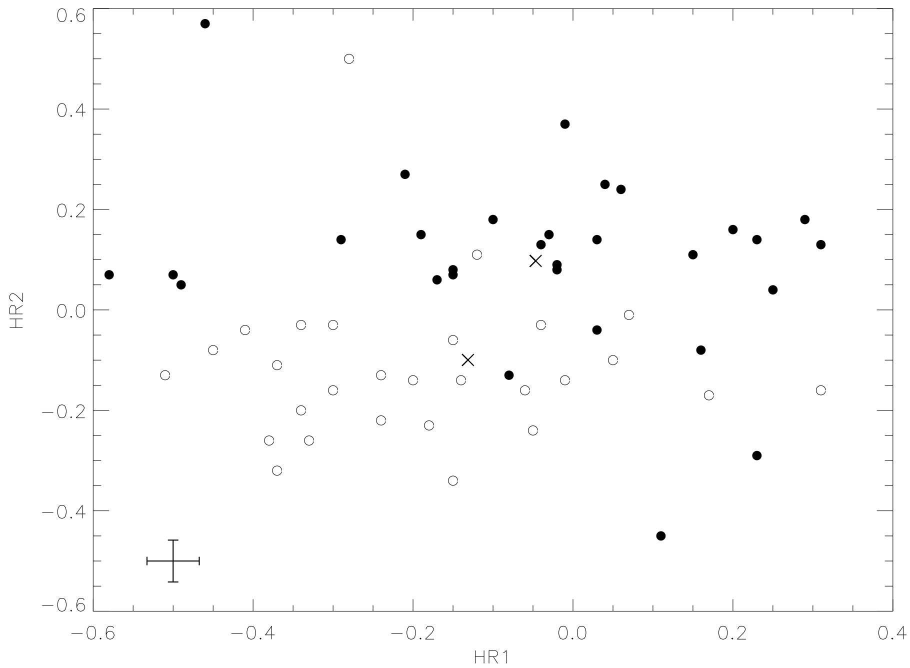

Figure 1: Hardness ratios (X-ray colors, $HR2$ versus $HR1$) for only flare radiation (filled circles) and corresponding stars in an inactive state (open circles) of the *ROSAT* PSPC observations of the UV Cet type stars. (x) – are corresponding to the mean values of each sample. Typical error bars are shown bottom left

In addition, all of the spectra mentioned above have been fitted also with a combination of absorbed thermal emission model using the MEKAL code as implemented in XSPEC, implementing the optically thin, collisional ionization equilibrium emissivity model described in Mewe *et al.* [23]. Everywhere, the presence of absorbing material has been accounted for using a WABS component in XSPEC and the global metal abundance has been left free, while abundance ratios were kept fixed in the fitting process. These abundance values are determined as relative to the "solar" case.

The results are clearly indicating, *in all cases*, an increase of coronal metal abundances at flare maximum (see Sciortino *et al.* [21], Favata & Schmitt [24]).

It should be noted that an acceptable fit also may be achieved with the two temperature (2-T) RS model holding metallicity abundance at the solar value.

2. CONCLUSIONS

We have analyzed *ROSAT* pointed (PSPC and HRI) as well as All Sky Survey data for flare detection on the UV Cet type flare stars of the solar vicinity. During the monitoring time of $\sim$ 1350 hours, the 160 flares or variations were detected using a Bayesian approach for change point detection.

It should be noted that all variations detected by the method have an high significant level (at least one of the detected change points has a posterior probability more than 0.9973).

Of course, all of these variations can not be connected with flares. X-ray brightness level in different Bayesian blocks sometimes could be associated with spots covered on the surface of a star.

Tight statistical correlations are observed between radiated flare luminosities in different X-ray bands.

On average, the radiation during flares is harder than in the quiescent state of a star.

Time resolved X-ray spectroscopy for some of the flares (under assumption of a 1T-model hot, optically thin plasma) clearly indicates an increase of coronal metallicity abundance at flare maximum.

Acknowledgments. VH wishes to acknowledge the warm hospitality of Professor J. Trümper and the Max-Planck-Institut für Extraterrestrische Physik during his stay as a Visiting Fellow. ROSAT is supported by the German government (BMBF/DLR) and the Max-Planck-Society. This project was supported by the Bundesministerium für Bildung und Forschung through the Deutsches Zentrum für Luft- und Raumfahrt E. V. (DLR) under grant number 50 OR 9706 8 and 50 OR 0003. The responsibility for the content of the publication lies with the authors.

REFERENCES

[1] *Gershberg R. E., Katsova M. M., Lovkaya M. N., et al.* Catalogue and bibliography of the UV Cet-type flare stars and related objects in the solar vicinity // Astron. and Astrophys.–1998.–**139**.–P. 555.

[2] *Scargle J.* // Astrophys. J.–1998.–**504**.–P. 405.

[3] *Mirzoyan L. V.* // Optical flares: Observations and Interpretation: Proc. IAU Coll. N 151 / Eds J. Greiner, H. W. Duerbeck and R. E. Gershberg.–Springer, 1995.–P. 47.

[4] *Montmerle T.* // Eds G. Micela, R. Pallavicini, S. Sciortino.–Mem. Soc. Astron. Ital.–**68**, N 4.–Soc. Astron. Ital., Firenze, 1997.–P. 1017.

[5] *Haisch B. M.* // Activity in Red Dwarf Stars / Eds P. B. Byrne, M. Rodonó.–Astrophys. and Speace Sci. Lib.–1983.–**102**.–P. 255.

[6] *Pallavicini R., Stella R., Tagliaferri G.* // Astron. and Astrophys.–1990.–**228**.–P. 443.

[7] *Schmitt J. H. M. M.* // Astrophys. J. Suppl. Ser.–1994.–**90**.–P. 735.

[8] *Cash W.* // Astrophys. J.–1979.–**228**.–P. 939.

[9] *Scargle J. D., Bapu G. J.* Point Processes in Astronomy: Exciting Events in the Universe // preprint, 1998, available at *http://ccf.arc.nasa.gov/˜scargle/hand_www.ps*

[10] *Trümper J.* // Adv. Space Res.–1982.–**2**, N 4.–P. 241.

[11] *Pfeffermann E., et al.* // Proc. SPIE.–1986.–**733**.–P. 519.

[12] *Hambaryan V., Neuhäuser R., Stelzer B.* // Astron. and Astrophys.–1999.–**345**.–P. 121 (HNS).

[13] *Zimmermann H. U., Boese G., Becker W., et al.* // EXSAS Users Guide, MPE Report, *ROSAT* Scientific Data Center, Garching, 1998.

[14] *Neuhäuser R., Sterzik M. F., Schmitt J. H. M. M., et al.* // Astron. and Astrophys.–1995.–**297**.–P. 391.

[15] *Cruddace R. G., Hasinger G. R., Schmitt J. H. M. M.* // Astronomy from Large Databases: ESO Conf. and Workshop Proc. 28 / Eds F. Murtagh, A. Heck.–Garching, 1988.–P. 177.

[16] *Jaynes E. T.* // Probability Theory: The Logic of Science, 1997, available at *http://bayes.wustl.edu*

[17] *Jeffreys H.* Theory of Probability, (3rd ed.), Oxford University Press, 1961.

[18] *Raftery A. E.* // Bayesian Model Selection in Social Research, University of Washington, preprint, 1994, available at *http://www.stat.washington.edu/raftery/Research/Bayes/bayes_papers.html*

[19] *Raymond J. C., Smith B. S.* // Astrophys. J. Suppl. Ser.–1977.–**35**.–P. 419.

[20] *Morrison R., McCammon D.* // Astrophys. J.–1983.–**270**.–P. 119.

[21] *Sciortino S., Maggio A., Favata F., Orlando S.* // Astron. and Astrophys.–1999.–**342**.–P. 502.

[22] *Schmitt J. H. M. M., Stern R.A., Drake J.J., Kürster M.* // Astrophys. J.–1996.–**464**.–P. 898.

[23] *Mewe R., Gronenschild E. H. B. M., van den Oord, G. H. J.* // Astron. and Astrophys.–1985.–**62**.–P. 197.

[24] *Favata F., Schmitt J. H. M. M.* // Astron. and Astrophys.–1999.–**350**.–P. 900.